elimination from **5** probably occurs. It should be pointed out that for the related cyclopentylidene case, CO_2 and the methyleneketene started appearing at 770 K, and this result was accounted for by a similar competitive CO_2 and acetone elimination directly from Meldrum's acid derivative.[25]

Finally it should be mentioned that for (methoxymethylene)-ketenes, no cyclization to the furan-3(2*H*)-one has ever been reported, although it is well-known that ((alkylthio)methylene)-[9] or ((alkylamino)[23,24] methylene)ketenes are quantitatively transformed into thiophen-3(2*H*)-ones and pyrrol-3(2*H*)-ones, respectively. The SPE spectra obtained from **5** do not support the formation of 5-methylfuran-3(2*H*)-one: for this heterocycle the band corresponding to the ionization of the carbonyl oxygen lone pair is expected, as in cyclopenten-2-one[22,26] around 9.35 eV. The interacting double bond and the intracyclic oxygen should give ($\pi - n_O$) and ($\pi + n_O$) orbitals. The IP's arising from the ejection of an electron from these two orbitals are not easily anticipated and could be compared, at first sight, to those of the methyl vinyl ether (**15**) at 9.15 and 12.13 eV.[13] If we exclude the spectrum of the methyleneketene **7** (Figures 1e and 2), the other observed pyrolyzate spectra are not consistent with such a structure.

Conclusion

In conclusion, the assignments of the PE spectra of substituted methyleneketenes are consistent with the previous results of Bock[6] and McNaughton[5] and confirm the formation of these highly unstable methyleneketenes from the pyrolysis of Meldrum's acid derivatives between 700 and 850 K. However when the double bond of the Meldrum's acid derivative is substituted by a methyl group, other intermediary pyrolysis products are observed at lower (730 K) or higher (920 K) temperatures for the methoxy compounds. The assignment of the PE spectra of the obtained products supports the formation of substituted vinylketene, in agreement with Wentrup's mechanism.[7]

However the different behavior of methoxy-substituted alkylidene derivatives of Meldrum's acid from that of alkylthio and alkylamino compounds, which readily cyclize when possible to thiophen-3(2*H*)-one and pyrrol-3(2*H*)-one, respectively, is not yet well understood. Further investigation is being undertaken.

Experimental Section

PE spectra were recorded on an Helectros 0078 spectrometer connected to a microcomputer system supplemented by a digital analogic converter (DAC). The spectrometer is equipped with an internal heating device for the SPP[10] (pressure in the ionization chamber: 10^{-5} mbar without sample). For the EP, the spectrometer is connected to a vacuum device where the pyrolysis is performed (pressure in the oven. 10^{-3} mbar without sample). The spectra are built with 2048 points and are accurate within 0.05 eV. They are calibrated on the known ionizations of xenon (12.13 and 13.43 eV) and argon (15.76 and 15.93 eV).

The starting Meldrum's acid derivatives **4** and **5** were prepared following Polansky's method[27] and the dithiocompound **8** according to Huang's synthesis.[28]

MNDO calculations were performed with the AMPAC program[29] on a VAX computer. All the geometries were fully optimized.

Acknowledgment. We thank Mrs. Maryse Simon for efficient technical assistance.

(22) Kimura, K.; Katsumata, S.; Achiba, Y.; Yamazaki, T.; Iwata, S. *Handbook of Hel Photoelectron Spectra of Fundamental Organic Molecules.* Japan Scientific Societies Press: Tokyo Halsted Press: New York, 1981.
(23) McNab, H.; Monahan, L. C. *J. Chem. Soc., Perkin Trans 1* **1988**, 863.
(24) Lorenčak, P.; Pommelet, J. C.; Chuche, J.; Wentrup, K. *J. Chem. Soc., Chem. Commun.* **1986**, 369.
(25) Wentrup, C.; Gross, G.; Bestermann, H. M.; Lorenčak, P. *J. Org. Chem.* **1985**, *50*, 2877.
(26) Chadwick, D.; Frost, D. C.; Weiler, L. *J. Am. Chem. Soc.* **1971**, *93*, 4320.
(27) Binlmayer, G. A.; Derflinger, G.; Derkosch, J.; Polansky, O. E. *Monatsch. Chem.* **1967**, *98*, 564.
(28) Huang, X.; Chen, B. C. *Synthesis* **1986**, 967.
(29) Dewar, M. J. S.; Stewart, J. J. P. *Quantum Chem. Prog. Exchange Bull.* **1986**, *6*, 24.

Metastable Unimolecular and Collision-Induced Dissociation of Hydrogen-Bonded Clusters: Evidence for Intracluster Molecular Rearrangement and the Structure of Solvated Protonated Complexes

S. Wei, W. B. Tzeng, R. G. Keesee, and A. W. Castleman, Jr.*

Contribution from the Department of Chemistry, The Pennsylvania State University, University Park, Pennsylvania 16802. *Received August 7, 1990. Revised Manuscript Received November 9, 1990*

Abstract: A reflectron time-of-flight mass spectrometer in conjunction with multiphoton ionization was used to study metastable unimolecular and collision-induced dissociation processes of mixed ammonia–pyridine and water–acetone cluster ions. The ion intensity distributions display especially stable pertuberances (magic numbers) at $m = n + 2$ for $(H_2O)_n{\cdot}(C_3H_6O)_mH^+$ and $m = 2(n + 1)$ for $(NH_3)_n{\cdot}(C_5H_5N)_mH^+$, indicating that the core ions are H_3O^+, $H_5O_2^+$, NH_4^+, etc. whenever the cluster size is large enough to form a closed hydrogen-bonded shell structure. Surprisingly, these core ions form even though the proton affinity of water is smaller than that of acetone, and that of ammonia is smaller than that of pyridine. Collision-induced dissociation is studied to probe structure (core ion) changes with cluster size. The structural changes are well-correlated to transitions of the metastable decomposition channels of these mixed cluster ions, and this correlation is successfully applied to other mixed cluster systems including ammonia–trimethylamine and water–dimethyl ether. Metastable decomposition studies show that the mixed cluster ions $H_2O{\cdot}(C_3H_6O)_3H^+$ and $NH_3{\cdot}(C_5H_5N)_3H^+$ lose H_2O and NH_3 molecules, respectively, which results from intracluster molecular rearrangement. This intracluster molecular rearrangement is confirmed by detailed investigations of the dynamics of metastable unimolecular and collision-induced dissociation processes.

Introduction

Clusters offer a means by which to bridge the gap between the gaseous and condensed phase so that the details of solvation as well as condensation and nucleation phenomena can be probed at the molecular level.[1-4] Research into the formation and properties of clusters has been rapidly expanding in recent years.[5-10]

(1) Jortner, J. *Ber. Bunsenges. Phys. Chem.* **1984**, *88*, 188.

0002-7863/91/1513-1960$02.50/0

Table I. Molecular Proton Affinities, Dipole Moments, and Polarizabilities

molecule	PA,[a] kcal/mol	μ,[b] D	α,[c] Å^3
H_2O	166.5	1.85	1.48
CH_3COOH	190.2	1.74	
CH_3COCH_3	196.7	2.88	6.33
NH_3	204.0	1.47	2.26
C_5H_5N	220.8	2.19	9.53
$(CH_3)_3N$	225.1	0.61	7.76

[a] Proton affinity, taken from ref 27a. [b] Dipole moment, taken from ref 27b. [c] Polarizability, calculated from $\alpha = 3(n_D^2 - 1)M(4\pi(n_D^2 + 2)\rho N_A)^{-1}$.

Although various techniques are available, multiphoton ionization in conjunction with reflectron time-of-flight mass spectrometry (R-TOFMS) has been found to be a particularly useful method in studies of the formation, bonding, structure, and detailed mechanisms of intracluster ion–molecule reactions in molecular and ionic clusters.[11-17]

For cluster ions (A)·(B)·H$^+$, Cooks and co-workers were the first to point out studies of metastable decomposition could yield information on relative proton affinities based on the argument of competitive shift,[7,18] i.e. the ability of the lowest energy channel to influence the metastable peak intensity for competing processes. For mixed cluster ions $(M)_m(N)_nH^+$ ($n + m < 25$), Stace and co-workers[7] found that it has been possible to determine which of the species present in the ion cluster is preferentially bound to the proton by monitoring the competitive decomposition process via the metastable peak intensities. It should be noted that for very large cluster ions, the assumption of competitive shift might not be applicable since at the threshold the rate constant for decomposition is commensurate with the detection time window associate with metastable detection; however, very large clusters are not the subject of the present study.

Collision-induced dissociation (CID) of high kinetic energy ions (keV) is a useful tool for determining the ion structure in general[21] and more specifically also for ion clusters whose fragmentations have been rationalized[22,23] by using the "instantaneous" dissociation model. In a general case, one assumes that there are two dissociation channels available to an activated cluster ion. The lower activation energy channel involves isomerization and requires passage over a isomerization barrier prior to dissociation. The higher activation energy corresponds to direct cleavage.[20] As transition states for isomerization are typically more restricted than those for simple bond cleavage, the state density at the isomerization barrier is lower than that at the transition state for bond cleavage. As a result, the unimolecular rate constant for simple bond cleavage increases faster with internal energy than that for isomerization.[20] At low internal energies, the cluster ion will dissociate predominately via the lower energy pathway of isomerization and subsequent dissociation. As the internal energy increases, the direct dissociation channel will increase.

Our earlier studies on mixed cluster ions of the form $(NH_3)_n·(B)_mH^+$ (where B is only a proton acceptor but not the proton donor) showed that NH_4^+ is the central species for all cluster size whenever B has lower proton affinity than NH_4^+ (e.g. acetone, acetonitrile, and acetaldehyde).[19,24,25] When B has higher proton affinity than NH_4^+ (such as trimethylamine), the results showed B is bonded to the proton more strongly than ammonia for the small clusters. However, interestingly the findings indicated that the core ion switches to NH_4^+, $N_2H_7^+$, and $N_3H_{10}^+$ for large clusters and the hydrogen-bonding shells are completed when $m = 2n + 2$, $n \leq 5$.[26] As an additional contribution in elucidating the transition in the nature of the protonated core of the cluster ions, a thorough study of metastable unimolecular and collision-induced dissociation of $(NH_3)_n·(M)_mH^+$ (M ≡ pyridine or trimethylamine) and $(H_2O)_n·(M)_mH^+$ (M ≡ acetone) was performed by the reflectron TOFMS method. The results of the findings for these systems, which were chosen because of the differing proton affinities and other molecular constants (see Table I), are reported herein.

Experimental Section

The apparatus used in these studies has been described in detail elsewhere.[15,16] The only modification is an addition of a cylindrical cell (i.d. 15 mm, length 25 mm) with two changeable apertures (4-mm diameter in the present study). Neutral clusters are formed by coexpanding through a pulsed nozzle (diameter = 150 μm) a gas mixture containing ammonia and pyridine or water and acetone vapors at a selected mixing ratio. Helium is used as the carrier gas. The base pressure of the source chamber is about 2×10^{-7} Torr. With the total stagnation pressure at 2400 Torr, the pressure is raised to no more than 2×10^{-6} Torr.

The neutral clusters are ionized by 355-nm light from a frequency-tripled Nd:YAG laser. Ions formed by the multiphoton ionization process are accelerated by a double electrostatic field to about 2.6 keV and thereafter pass through a collision cell located at a distance of 10 cm away from the ionization region. Thereafter they travel through a 120 cm long field-free region toward the reflectron. Ions are reflected back at an overall angle of 3° and travel 80 cm through another field-free region toward a chevron microchannel plate (MCP) detector. The signal

(2) Castleman, A. W., Jr.; Keesee, R. G. *Chem. Rev.* **1986**, *86*, 589. Castleman, A. W., Jr.; Keesee, R. G. *Acc. Chem. Res.* **1986**, *19*, 413. Castleman, A. W., Jr.; Keesee, R. G. *Science* **1988**, *241*, 36.
(3) Sugano, S., Nishina, Y., Ohnishi, S. Eds. *Microclusters*; Springer Series in Materials Science; Springer-Verlag: Berlin, 1987; Vol. 4.
(4) Jena, P., Rao, B. K., Khanna, S. N., Eds. *Physics and Chemistry of Small Clusters*: NATO ASI Series B; Plenum: New York, 1987; Vol. 158.
(5) Hwang, H. J., Senshama, D. K., El-Sayed, M. A. *J. Phys. Chem.* **1989**, *93*, 5012. Hwang, H. J.; Senshama, D. K., El-Sayed, M. A. *Chem. Phys. Lett.* **1989**, *160*, 243.
(6) Garvey, J.; Bernstein, R. B. *J. Phys. Chem.* **1986**, *90*, 3577. Garvey, J.; Bernstein, R. B. *Chem. Phys. Lett.* **1986**, *126*, 394. Garvey, J.; Bernstein, R. B. *J. Am. Chem. Soc.* **1986**, *108*, 6096; **1987**, *109*, 1921.
(7) Stace, A. J. *Mass Spectrom.* **1987**, *9*, 96. Stace, A. J.; Shulkla, A. K. *J. Am. Chem. Soc.* **1982**, *104*, 5314.
(8) Märk, T. D. *Int. J. Mass Spectrom. Ion Processes* **1987**, *79*, 1.
(9) DeHeer, W. A.; Knight, W. D.; Chou, M. Y.; Cohen, M. L. *Solid State Phys.* **1987**, *40*, 93.
(10) Squires, R. R. *Chem. Rev.* **1987**, *87*, 623.
(11) Boesl, U.; Neusser, H. J.; Weinkauf, R.; Schlag, E. W. *J. Phys. Chem.* **1982**, *86*, 4857.
(12) Kuhlewind, H.; Neusser, H. J.; Schlag, E. W. *Int. J. Mass Spectrom. Ion Processes.* **1983**, *51*, 255.
(13) Echt, O.; Morgan, S.; Dao, P. D.; Stanley, R. J.; Castleman, A. W., Jr. *Ber. Bunsengen. Phys. Chem.* **1984**, *88*, 217.
(14) Morgan, S.; Castleman, A. W., Jr. *J. Am. Chem. Soc.* **1987**, *109*, 2867. Morgan, S.; Castleman, A. W., Jr. *J. Phys. Chem.* **1989**, *93*, 4544.
(15) Breen, J. J.; Kilgore, K.; Tzeng, W. B.; Wei, S.; Keesee, R. G.; Castleman, A. W., Jr. *J. Chem. Phys.* **1989**, *90*, 11.
(16) Tzeng, W. B.; Wei, S.; Castleman, A. W., Jr. *J. Am. Chem. Soc.* **1989**, *111*, 6035.
(17) Wei, S.; Tzeng, W. B.; Castleman, A. W., Jr. *J. Chem. Phys.* **1990**, *92*, 336.
(18) Cooks, R. G.; Beynon, J. H.; Caprioli, R. M.; Lester, G. R. *Metastable Ions*; Elsevier: Amsterdam, 1973. Cooks, R. G.; Kruger, T. L. *J. Am. Chem. Soc.* **1977**, *99*, 1279.
(19) Tzeng, W. B.; Wei, S.; Castleman, A. W., Jr. *Chem. Phys. Lett.* **1990**, *166*, 343.
(20) Forst, W. *Theory of Unimolecular Reactions*; Academic Press: New York, 1973.
(21) Levsen, K.; Schwarz, H. *Mass Spec. Rev.* **1983**, *2*, 77. Bouma, W. L.; MacLeod, J. K.; Radom, L. *J. Am. Chem. Soc.* **1982**, *104*, 2930. Holmes, J. L.; Lossing, F. P.; Terlouw, J. K.; Burgers, P. C. *J. Am. Chem. Soc.* **1982**, *104*, 2931.
(22) Freas, R. B.; Dunlap, B. I.; Waite, B. A.; Campana, J. E. *J. Chem. Phys.* **1987**, *86*, 1276. Graul, S. T.; Squires, R. R. *Int. J. Mass Spectrom. Ion Processes* **1989**, *94*, 41.
(23) Iraqi, M.; Lifshitz, C. *Int. J. Mass Spectrom. Ion Processes* **1986**, *71*, 245; **1989**, *88*, 45.
(24) Tzeng, W. B.; Wei, S.; Neyer, D. W.; Keesee, R. G.; Castleman, A. W., Jr. *J. Am. Chem. Soc.* **1990**, *112*, 4097.
(25) Tzeng, W. B.; Wei, S.; Castleman, A. W., Jr. Stability and Structures of Solvated Cluster Ions: Ammonia-Acetonitrile and Ammonia-Acetaldehyde Systems. *J. Phys. Chem.*, submitted.
(26) Wei, S.; Tzeng, W. B.; Castleman, A. W., Jr. The Structure of Protonated Solvation Complexes: Ammonia-Trimethylamine Cluster Ions, and Their Metastable Decompositions. *J. Phys. Chem. J. Phys. Chem.* **1991**, *95*, 585.
(27) (a) Lias, S. G.; Liebman, J. F., Levin, R. D. *J. Phys. Chem. Ref. Data* **1984**, *13*, 695. (b) Nelson, R. D., Jr.; Lide, D. R., Jr.; Maryott, A. A. *Selected Values of Electric Dipole Moments for Molecules in the Gas Phase*; NSRDS-NBS, Washington D.C., 1967.

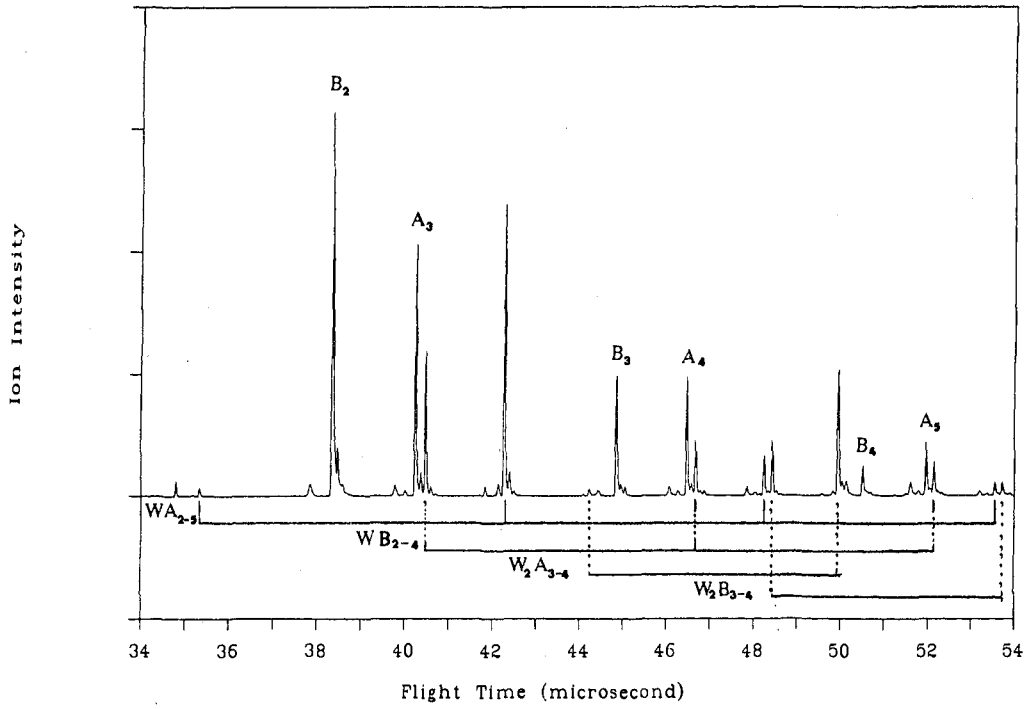

Figure 1. Hard reflection TOF spectra of the mixed water–acetone system (liquid mixing ratio of acetone/water = 1/100) taken at U_t = 2800 V (U_0 = 2600 ± 10 V): $A_m \equiv (C_3H_6O)_mH^+$, $B_m \equiv (C_3H_6O)_m{\cdot}CH_3CO^+$, $W_nA_m \equiv (H_2O)_n{\cdot}(C_3H_6O)_mH^+$, $W_nB_m \equiv (H_2O)_n{\cdot}(C_3H_6O)_m{\cdot}CH_3CO^+$.

received by the MCP is fed into a 100-MHz transient recorder coupled to an IBM PC/AT microcomputer. The experiments operate at 10 Hz and TOF spectra typically are accumulated for 2000 laser shots.

The pressures in the drift field-free and detector regions are maintained at 2×10^{-7} Torr during normal operation. In conducting the metastable unimolecular dissociation studies, experiments are performed to ensure that collision-induced dissociation of the cluster ions is negligible[16,17] under the conditions selected for the measurements. The parent ion birth potential U_0, established by the voltages applied to the TOF lens elements, was measured to be 2600 ± 10 V in the present study. A hard reflection time-of-flight (TOF) spectrum[16,17] can be obtained when the voltage applied to the middle plate of the reflectron unit (U_t) is set higher than the initial parent ion energy (U_0). When a metastable decomposition process occurs in the field-free region, the daughter ion has an energy of $(M_d/M_p)U_0$, where M_d and M_p are the daughter ion and parent ion mass. The daughter ion spectrum can be obtained when U_t is set lower than U_0 but higher than $(M_d/M_p)U_0$.

Under typical CID experimental conditions, the collision cell pressure is on the order of 10^{-4} Torr when the flow rate of the collision gas (nitrogen) is about 0.02 standard cubic centimeters per minute (sccm). In this case the source chamber pressure is raised from 2×10^{-6} to 4×10^{-6} Torr while the detection chamber is raised from 2×10^{-7} to 5×10^{-7} Torr.

The ammonia (anhydrous, minimum purity of 99.99%) used in these experiments was obtained from Linde Specialty Gases, whereas the pyridine (purity of 99.0%) and trimethylamine (purity of 99.0%) were obtained from Aldrich Chemical Co. These compounds were used without further purification.

Results

A. Mixed Water–Acetone System. (1) Hard Reflection Time-of-Flight Spectrum. After multiphoton ionization of neat acetone clusters, two major cluster ion series, $(C_3H_6O)_mH^+$ and $(C_3H_6O)_m{\cdot}CH_3CO^+$ and a minor series, $(C_3H_6O)_m{\cdot}CH_3^+$, are produced.[16] Similarly, two major mixed cluster ion series, $(H_2O)_n{\cdot}(C_3H_6O)_mH^+$ and $(H_2O)_n{\cdot}(C_3H_6O)_m{\cdot}CH_3CO^+$, are observed after multiphoton ionization of mixed neutral water–acetone clusters as seen in Figure 1. The ion intensity distributions of $(H_2O)_n{\cdot}(C_3H_6O)_mH^+$, n = 1–6, are plotted as a function of m in Figure 2. When $n \leq 4$, magic numbers at $m = n + 2$ are clearly seen. When $n > 4$, however, the pattern begins to break down. The cluster ion series, $(H_2O)_n{\cdot}(C_3H_6O)_m{\cdot}CH_3CO^+$ also gives similar results. The ion intensity distributions of $(H_2O)_n{\cdot}(C_3H_6O)_m{\cdot}CH_3CO^+$, n = 1–6, are plotted as a function of m in Figure 3. Magic numbers at $m = n + 1$ are evident when $n \leq$ 4. However, the pattern of $m = n + 1$ does not hold when $n >$ 4. This finding was further confirmed in the present study under various experimental conditions, e.g. nozzle stagnation pressure (1000–5000 Torr), laser power (10–40 mJ/pulse), and the mixing ratio of acetone to water (from 10/1 to 1/200). The general features in the cluster ion distribution (i.e. magic numbers) are independent of experimental conditions mentioned above.

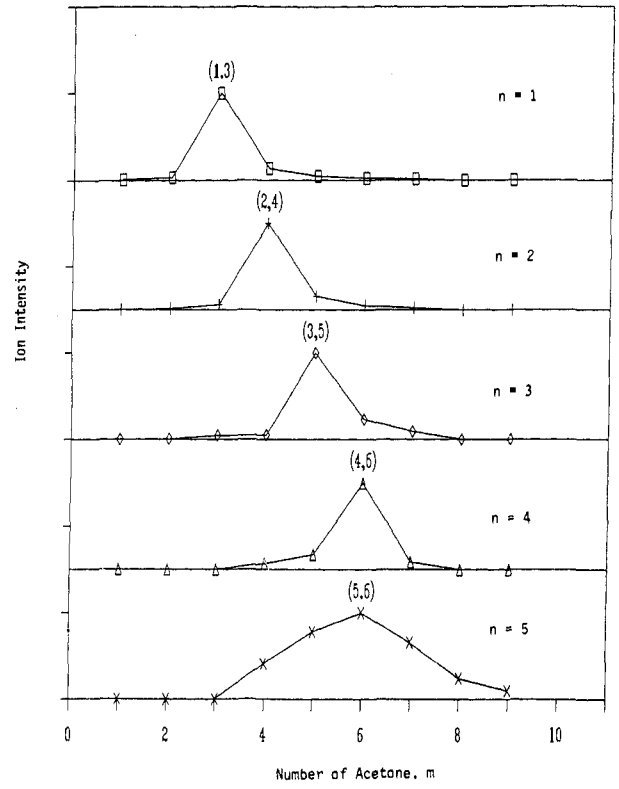

Figure 2. The intensity distribution of $(H_2O)_n{\cdot}(C_3H_6O)_mH^+$ as a function of m. Magic numbers at $m = n + 2$ are seen when $n \leq 4$. When n = 5, the most intense peak is at m = 6.

(2) Metastable Unimolecular Decomposition. A small difference in the flight times of the daughter ion and its parent (a few tenths

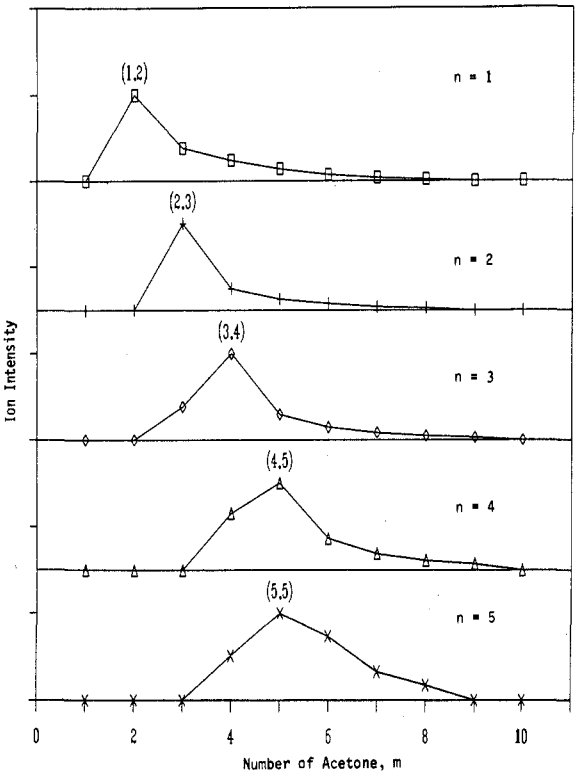

Figure 3. The intensity distribution of $(H_2O)_n{\cdot}(C_3H_6O)_m{\cdot}CH_3CO^+$ as a function of m. Magic numbers at $m = n + 1$ are seen when $n \leq 4$. When $n = 5$, the magic number is at $m = 5$.

of a microsecond) arises from their slightly different flight paths in the reflectron. This allows one to assign the metastable ion peaks by simply comparing the arrival times of daughter and parent ions in the TOF spectra. In order to further confirm the identification of daughter ions, we also apply an ion cut-off potential method[16,19] which involves observing the presence/absence of daughter ion peaks upon changing the voltage settings on the middle plate of the reflectron unit (U_t).

In general, there are two possible metastable decomposition channels for the mixed cluster ion $(H_2O)_n{\cdot}(C_3H_6O)_mH^+$:

$$(H_2O)_n{\cdot}(C_3H_6O)_mH^+ \rightarrow (H_2O)_{n-1}{\cdot}(C_3H_6O)_mH^+ + H_2O \quad (1)$$

$$(H_2O)_n{\cdot}(C_3H_6O)_mH^+ \rightarrow (H_2O)_n{\cdot}(C_3H_6O)_{m-1}H^+ + C_3H_6O \quad (2)$$

For a parent cluster ion of mass M_p, the corresponding daughter ion masses are $(M_p - 18)$ for process 1 and $(M_p - 58)$ for process 2, respectively. As described in the Experimental Section, the daughter ions have energies of $[(M_p - 18)/M_p]U_0$ and $[(M_p - 58)/M_p]U_0$. Here, we apply the daughter ion cutoff potential method for investigation of the three possible metastable decomposition mechanisms: (a) both channels coexist, (b) only channel 1 is open, and (c) only channel 2 is open.

If two channels open simultaneously, two daughter ion peaks will appear in the daughter ion spectrum for a corresponding parent ion. The separation of these two peaks in the daughter ion TOF spectrum is determined by the following equation:

$$\Delta t = C(U_0/M_p)^{1/2}(M_{d1} - M_{d2})/U_t \quad (3)$$

where M_{d1} and M_{d2} are the masses of the two daughter ions from the same parent ion as indicated in processes 1 and 2. The constant C equals $(2.88L)q^{-1/2}$ (L = 1.5 cm, the distance of the first grid and the middle grid of the reflectron unit) with Δt in μs, M_p, M_{d1}, and M_{d2} in amu, U_0 and U_t in V, and q in units of elementary charge. As an example, for parent ion $H_2O{\cdot}(C_3H_6O)_3H^+$ (M_p = 193 amu) with an energy of 2600 eV, the daughter ion energies are 2358 and 1819 eV for channels 1 and 2, respectively. If the two channels are open simultaneously, two daughter ion peaks for parent ion $H_2O{\cdot}(C_3H_6O)_3H^+$ will be separated by 0.25 μs at U_t = 2550 V. This can be easily identified with our apparatus which has a TOF resolution better than 0.02 μs (mass resolution $m/\Delta m$ = 1200) in the mass range of 200.

If the metastable decomposition only follows channel 1, the daughter ion peak will disappear when U_t is below 2358 V. However, if the daughter ion peak persists, one may propose that channel 2 is the only possible metastable decomposition process. Whether channel 2 is the only possible metastable decomposition process can be further confirmed by observing the disappearance

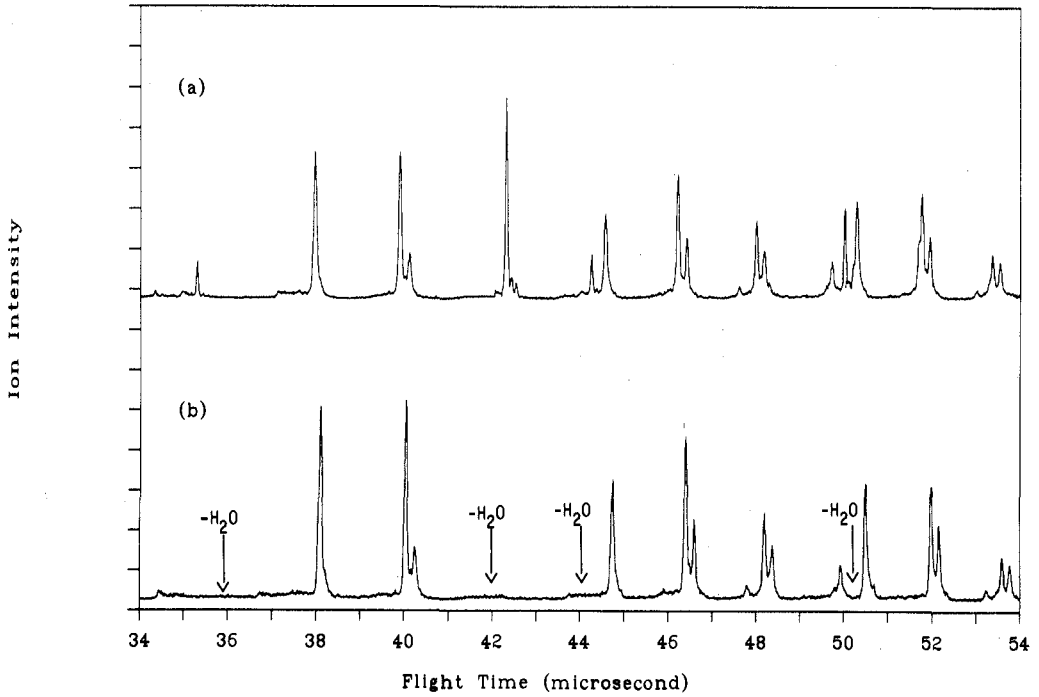

Figure 4. The metastable daughter ion spectra of the mixed water–acetone system at different U_t settings showing the cutoff method: (a) at U_t = 2550 V, their parent showing in Figure 1 (only $(H_2O)_2{\cdot}(C_3H_6O)_4H^+$ gives two metastable channels); (b) at U_t = 2200 V, four daughter peaks with loss of water are gone (these metastable processes are $H_2O{\cdot}(C_3H_6O)_2H^+ \rightarrow (C_3H_6O)_2H^+ + H_2O$, $H_2O{\cdot}(C_3H_6O)_3H^+ \rightarrow (C_3H_6O)_3H^+ + H_2O$, $(H_2O)_2{\cdot}(C_3H_6O)_3H^+ \rightarrow H_2O{\cdot}(C_3H_6O)_3H^+ + H_2O$, and $(H_2O)_2{\cdot}(C_3H_6O)_4H^+ \rightarrow H_2O{\cdot}(C_3H_6O)_4H^+ + H_2O$).

Table II. Metastable Decomposition of $(H_2O)_n(C_3H_6O)_mH^+$ and $(H_2O)_n(C_3H_6O)_mCH_3CO^+$ As Determined from the Cutoff Method[a]

m, C_3H_6O	n. H_2O 1	2	3	4
	(a) $(H_2O)_n(C_3H_6O)_nH^+$			
1	$-H_2O$			
2	$-H_2O$			
3	$-H_2O$	$-H_2O$		
4	-T	$-H_2O$,-T		
5	-T	-T	-T	
6	-T	-T	-T	-T
7	-T	-T	-T	-T
8	-T	-T	-T	-T
	(b) $(H_2O)_n(C_3H_6O)_mCH_3CO^+$			
1				
2	-T			
3	-T	-T		
4	-T	-T	-T	
5	-T	-T	-T	-T
6	-T	-T	-T	-T
7	-T	-T	-T	-T
8	-T	-T	-T	-T

[a] $-H_2O$ denotes loss of water and -T denotes loss of acetone.

of the daughter ion peak as U_t is lowered to a value less than 1819 V.

Figure 4 displays the typical daughter ion TOF spectra. The corresponding parent TOF spectrum is shown in Figure 1. Parts a and b of Figure 4 display the same portion of the daughter ion TOF spectrum at different U_t settings to demonstrate the cutoff potential method. The metastable channels of the series $H_2O\cdot(C_3H_6O)_mH^+$ are in agreement with observations of Stace et al.[28] They found that the cluster ions with the combination of $m = n + 2$ lose a water molecule, while the cluster ions with the combination $m > n + 2$ lose acetone. When comparing parts a and b of Figure 4 it can be seen that the daughter ion peaks in Figure 4a, corresponding to the parent ions $H_2O\cdot(C_3H_6O)_2H^+$ and $H_2O\cdot(C_3H_6O)_3H^+$, are gone at $U_t = 2200$ V in Figure 4b. This indicates that a water molecule is lost during metastable decomposition, while the daughter ion peaks corresponding to the parent ions $H_2O\cdot(C_3H_6O)_4H^+$ and $H_2O\cdot(C_3H_6O)_5H^+$ still exist, which indicates the loss of an acetone molecule. With the same combination of $m = n + 2$, the cluster ion $(H_2O)_2\cdot(C_3H_6O)_4H^+$ shows two channels open simultaneously while the cluster ion $(H_2O)_3\cdot(C_3H_6O)_5H^+$ loses an acetone molecule. In Figure 4a, two daughter ion peaks are seen for the parent ion peak $(H_2O)_2\cdot(C_3H_6O)_4H^+$ corresponding to loss of water and acetone. The assignment is proven by the cutoff method since one peak corresponding to the water loss is gone at $U_t = 2200$ V in Figure 4b while the other one corresponding to the acetone loss still exists. These are not due to collision-induced dissociation since no other cluster ions are found to give these two channels simultaneously. The complete results are summarized in Table II.

(3) Collision-Induced Dissociation of $H_2O\cdot(C_3H_6O)_3H^+$. Both theoretical[29] and experimental[22,23,30] studies suggest that H_3O^+ is the core ion in the cluster ion with the general form $H_2O\cdot(M)_3H^+$ (e.g. M ≡ CH_3CN, CH_3OCH_3). However, the metastable decomposition of the cluster ion $H_2O\cdot(C_3H_6O)_3H^+$ shows the channel involving the loss of a water molecule. In order to find out whether intracluster molecular rearrangement is involved during the metastable decomposition, the collision-induced dissociation of this cluster ion is examined.

Three decomposition channels (loss of a water molecule only, loss of an acetone molecule only, and simultaneous loss of both water and acetone molecules) are seen when introducing nitrogen as the collision gas. However, the water loss channel shows a different pressure dependence than the other two channels. In Figure 5 the dissociation fraction calculated from the integrated ion intensities of both parent and daughter ion peaks is plotted as a function of the collision gas pressure. It is seen that the water loss channel is pressure independent while the acetone loss channel increases as the pressure increases.

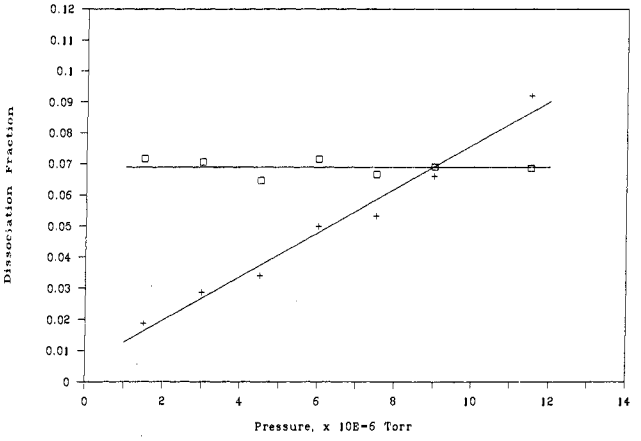

Figure 5. The pressure dependence of two dissociation channels from collision-induced dissociation studies: (□) $H_2O\cdot(C_3H_6O)_3H^+ \rightarrow (C_3H_6O)_3H^+ + H_2O$; (+) $H_2O\cdot(C_3H_6O)_3H^+ \rightarrow H_2O\cdot(C_3H_6O)_2H^+ + C_3H_6O$.

B. Mixed Ammonia–Pyridine System. (1) Hard Reflection Time-of-Flight Spectrum. In the multiphoton ionization of neutral ammonia–pyridine clusters, the observed major cluster ions are $(NH_3)_nH^+$, $(C_5H_5N)_mH^+$, and $(NH_3)_n\cdot(C_5H_5N)_mH^+$. A typical hard reflection TOF spectrum is shown in Figure 6. The experimental conditions and assignments are included in the figure captions. It has been known that the component ratio of the gas mixture is a crucial factor in producing the mixed cluster ions.[24,26,28,31] Varying the gas mixing ratio does affect the overall abundance distributions of the neutral clusters. In the present study we concentrate on the relative abundance of the mixed cluster ions $NH_3\cdot(C_5H_5N)_mH^+$ and the general trend of their size distribution.

Figure 7 displays the ion intensity distribution of $NH_3\cdot(C_5H_5N)_mH^+$ as a function of m, at different mixing ratios (R) = 50/1, 20/1, 1/1, and 1/10. A local minimum at $m = 2$ is evident despite the dramatic change of the gas component ratios of ammonia/pyridine from 50/1 to 1/10 and the magic number at $m = 4$ starts to show up at the mixing ratio of ammonia/pyridine = 1/10.

(2) Metastable Unimolecular Decomposition of $NH_3\cdot(C_5H_5N)_mH^+$. Metastable decomposition shows a switch in the loss channel between $m = 3$ to 4. When $m \leq 3$, cluster ions $NH_3\cdot(C_5H_5N)_mH^+$ lose an ammonia molecule; when $m \geq 4$, one pyridine molecule is lost. The typical daughter ion spectrum is shown in Figure 8. Parts a and b of Figure 9 display the same portion of daughter ion TOF spectra at different U_t settings to demonstrate the cutoff potential method. Three daughter ion peaks (labeled a, b, and c) in Figure 9a are identified to come from the parent ions $(C_5H_5N)_3H^+$, $NH_3\cdot(C_5H_5N)_3H^+$, and $NH_3\cdot(C_5H_5N)_4H^+$, respectively. As shown in Figure 9b, at $U_t = 2300$ V, peak b is gone, showing that an ammonia molecule is lost from $NH_3\cdot(C_5H_5N)_3H^+$. Observation of the disappearance of peaks a and c at various U_t indicates that a pyridine molecule is lost from their precursors. The decomposition fractions calculated from integrated parent and daughter ion intensities corresponding to these processes are listed in the following. The error bar of the reported values is about 10%.

$$(C_5H_5N)_3H^+ \rightarrow (C_5H_5N)_2H^+ + C_5H_5N \quad 7.0\% \quad (4)$$

$$NH_3(C_5H_5N)_3H^+ \rightarrow (C_5H_5N)_3H^+ + NH_3 \quad 10.7\% \quad (5)$$

$$NH_3(C_5H_5N)_4H^+ \rightarrow NH_3(C_5H_5N)_3H^+ + C_5H_5N \quad 11.9\% \quad (6)$$

(28) Stace, A. J.; Moore, C. J. *J. Phys. Chem.* **1982**, *86*, 3681.
(29) Mestdagh, J. M.; Binet, A.; Sublemontier, O. *J. Phys. Chem.* **1989**, *93*, 8300.
(30) Deakyne, C. A.; Meot-Ner, M.; Campbell, C. L.; Hugher, M. G.; Murphy, S. P. *J. Chem. Phys.* **1986**, *84*, 4958.
(31) Smith, D.; Adames, N. G.; Alge, E. *Planet. Space Sci.* **1981**, *29*, 449. Bohringer, H.; Arnold, F. *Nature (London)* **1981**, *290*, 321.

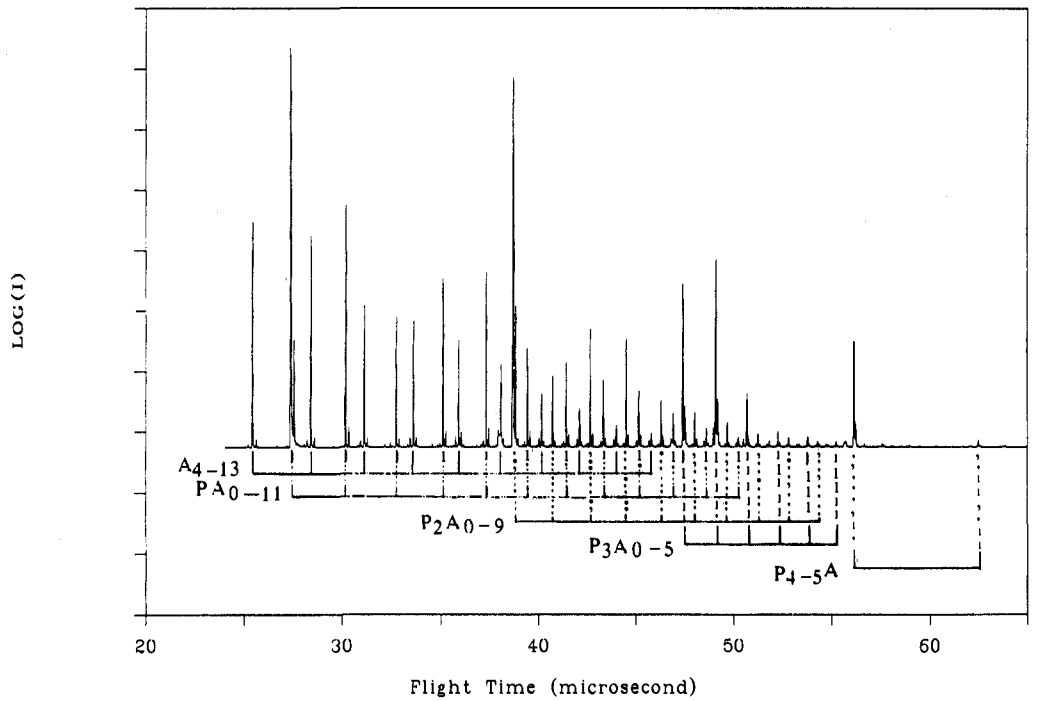

Figure 6. A hard reflection TOF spectrum of the mixed ammonia–pyridine system (gas mixing ratio R = ammonia/pyridine = 20/1) taken at U_t = 2800 V (U_0 = 2600 ± 10 V): $A_n \equiv (NH_3)_nH^+$, $P_mA_n \equiv (C_5H_5N)_m{\cdot}(NH_3)_nH^+$.

Table III. Metastable and CID Channels of $NH_3(C_5H_5N)_mH^+$ [a]

parent ion	metastable	CID
$NH_3(C_5H_5N)H^+$	$-NH_3$	$-NH_3$
$NH_3(C_5H_5N)_2H^+$	$-NH_3$	$-NH_3$
		$-NH_3 + C_5H_5N$
$NH_3(C_5H_5N)_3H^+$	$-NH_3$	$-NH_3$ [b]
		$-NH_3 + C_5H_5N$
		$-NH_3 + 2C_5H_5N$
$NH_3(C_5H_5N)_4H^+$	$-C_5H_5N$	$-C_5H_5N$
		$-NH_3 + 2C_5H_5N$
		$-NH_3 + 3C_5H_5N$
$NH_3(C_5H_5N)_5H^+$	$-C_5H_5N$	$-C_5H_5N$
		$-2C_5H_5N$
		$-NH_3 + 3C_5H_5N$
		$-NH_3 + 4C_5H_5N$

[a] $-NH_3$ denotes loss of ammonia; $-C_5H_5N$ denotes loss of pyridine; $-NH_3 + C_5H_5N$ denotes loss of ammonia and pyridine. [b] This channel is due to the metastable decomposition.

In the observable time window of 1–40 μs, all cluster ions $NH_3{\cdot}(C_5H_5N)_mH^+$ undergo unimolecular decomposition by losing either the ammonia or the pyridine neutral molecule. The complete metastable unimolecular dissociation processes of $NH_3{\cdot}(C_5H_5N)_mH^+$ are listed in Table III.

(3) Collision-Induced Dissociation of $NH_3{\cdot}(C_5H_5N)_mH^+$ and $(NH_3)_n{\cdot}((CH_3)_3N)_mH^+$. Parts a–d in Figure 10 are daughter ion TOF spectra under collision-induced dissociation (CID) conditions. Figure 10a is taken at U_t = 2550 V. As compared to the metastable daughter ion spectrum (Figure 9a), it is evident that more dissociation channels are open due to collision-induced dissociation. The assignment of each dissociation channel is done by the cutoff potential method as described in the previous section. At U_t = 2300 V (Figure 10b), peak e is clearly gone, indicating that the $NH_3{\cdot}(C_5H_5N)_3H^+$ loses NH_3 as a result of CID. At U_t = 1730 V (Figure 10c), peak b disappears, showing that $(C_5H_5N)_3H^+$ releases one pyridine after collision. Peak d still appears at the same intensity indicating that $NH_3{\cdot}(C_5H_5N)_3H^+$ does not lose a pyridine molecule (if so, it should have vanished at U_t = 1795 V). The cutoff potential of peak d is found at U_t = 1621 V as seen in Figure 10d. The process is identified as $NH_3{\cdot}(C_5H_5N)_3H^+$ losing pyridine and ammonia. The rest of the peaks are determined in the same way, and their identification is summarized in the figure caption. The dissociation fractions of each channel are shown below. The error bar of the reported value is about 15% at the constant flow (0.2 sccm) of the collision gas.

$$(C_5H_5N)_3H^+ \longrightarrow (C_5H_5N)_2H^+ + C_5H_5N \quad 14.2\% \quad (7)$$

$$\longrightarrow (C_5H_5N)H^+ + 2C_5H_5N \quad 7.1\% \quad (8)$$

$$NH_3(C_5H_5N)_3H^+ \longrightarrow (C_5H_5N)_3H^+ + NH_3 \quad 10.2\% \quad (9)$$

$$\longrightarrow (C_5H_5N)_2H^+ + NH_3 + C_5H_5N \quad 10.9\% \quad (10)$$

$$\longrightarrow C_5H_5NH^+ + NH_3 + 2C_5H_5N \quad 5.5\% \quad (11)$$

$$NH_3(C_5H_5N)_4H^+ \longrightarrow NH_3(C_5H_5N)_3H^+ + C_5H_5N \quad 18.0\% \quad (12)$$

$$\longrightarrow (C_5H_5N)_2H^+ + NH_3 + 2C_5H_5N \quad 9.5\% \quad (13)$$

$$\longrightarrow C_5H_5NH^+ + NH_3 + 3C_5H_5N \quad 4.2\% \quad (14)$$

The mixed ammonia–trimethylamine cluster ions have been studied.[26] It is found that the magic number pattern can be well-correlated to the core ions of NH_4^+, $N_2H_7^+$, $N_3H_{10}^+$, etc. to which the other trimethylamine molecules are hydrogen bonded. Collision-induced dissociation studies on this system were carried out in the present study. The complete CID results of $NH_3{\cdot}(C_5H_5N)_mH^+$ and $(NH_3)_n{\cdot}((CH_3)_3N)_mH^+$ are presented in Tables III and IV.

Discussion

A. Closed-Shell Structures of Hydrogen-Bonded Cluster Ions and Magic Numbers. The magic number patterns of the hydrogen-bonded cluster ions can be well-correlated to their closed-shell structures, a fact pointed out by ourselves[26] and others.[28] For example, $H_2O{\cdot}(C_3H_6O)_3H^+$ and $(H_2O)_2{\cdot}(C_3H_6O)_4H^+$ can be pictured as following ($T \equiv C_3H_6O$):

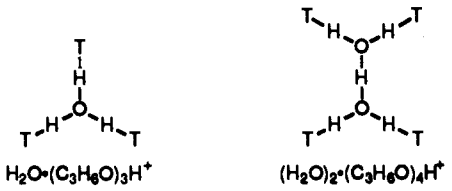

$H_2O{\cdot}(C_3H_6O)_3H^+$ $(H_2O)_2{\cdot}(C_3H_6O)_4H^+$

The maximum number of hydrogen-bonding sites on the core ion $(H_2O)_nH^+$ is $(n + 2)$ if a chain-like structure is assumed. Due to the formation of the closed hydrogen-bonded shell structures at these combinations, the magic number pattern of $m = n + 2$ for $(H_2O)_n{\cdot}(C_3H_6O)_mH^+$ is not surprising except for the fact that the proton affinity of water is so much less than that of acetone

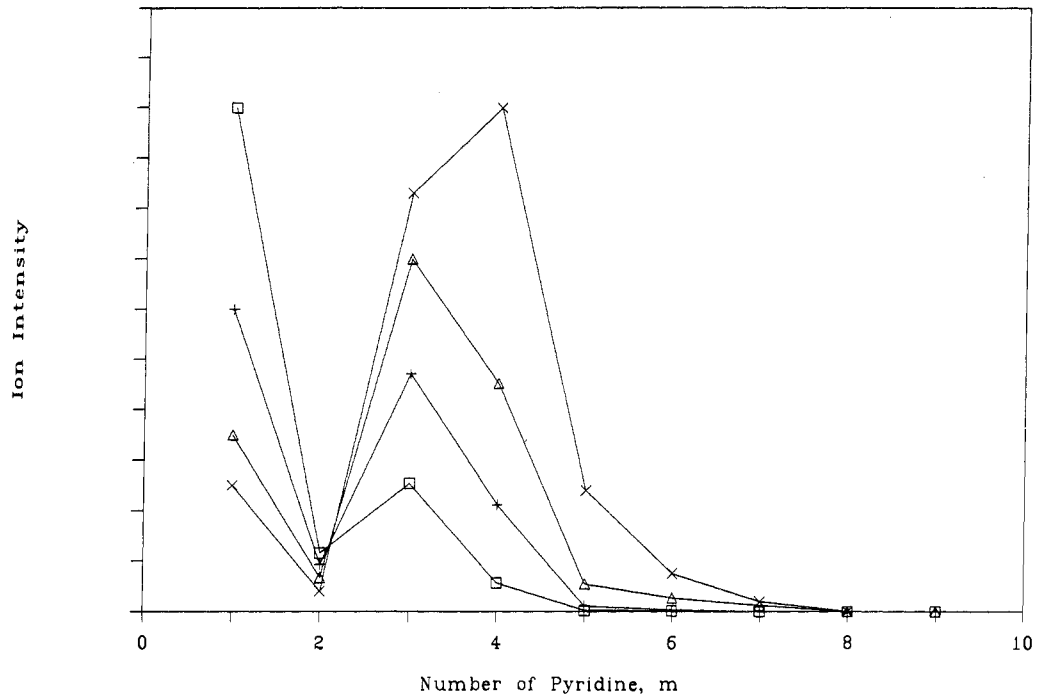

Figure 7. Ion intensity distribution of $NH_3{\cdot}(C_5H_5N)_mH^+$ with a local minimum at $m = 2$: (□) $R = 50/1$, (+) $R = 20/1$, (△) $R = 1/1$, (×) $R = 1/10$.

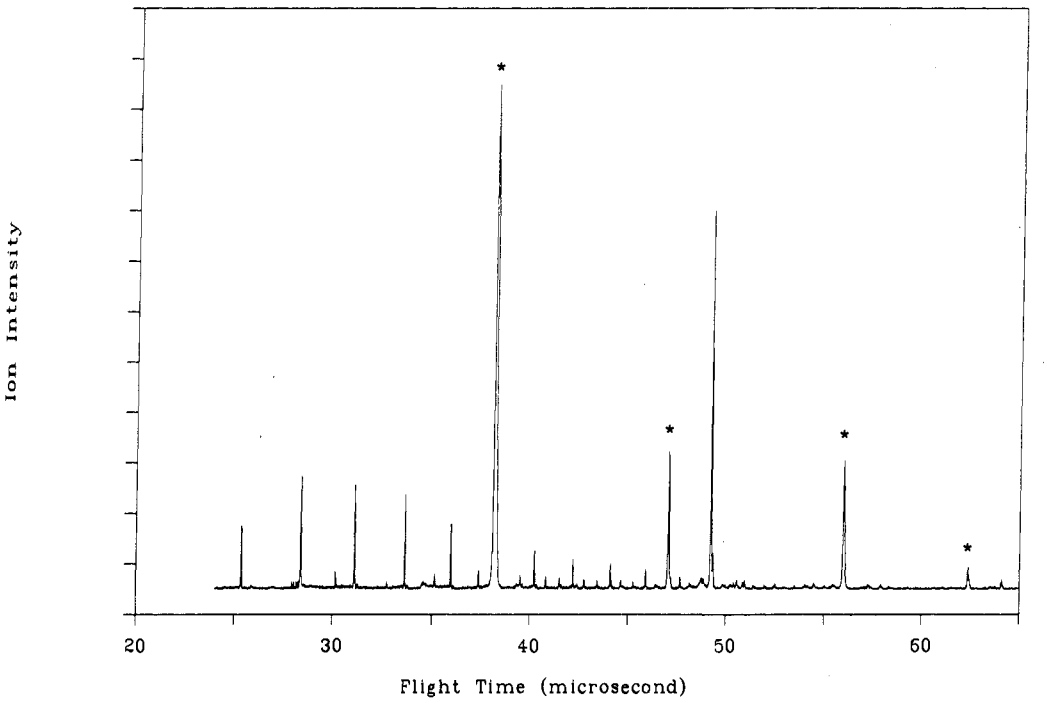

Figure 8. A metastable daughter ion TOF spectrum, $U_t = 2550$ V. The asterisk indicates that one pyridine molecule is lost in the metastable decomposition process and the corresponding parent ions are labeled according to those in Figure 6.

(166.5 compared to 196.7 kcal/mol). Similarly, the structures of $H_2O{\cdot}(C_3H_6O)_2{\cdot}CH_3CO^+$ and $(H_2O)_2{\cdot}(C_3H_6O)_3{\cdot}CH_3CO$ can be drawn as follows:

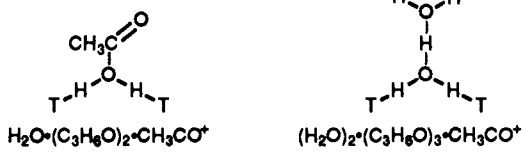

A similar pattern also has been found in the mixed ammonia–trimethylamine cluster ion system.[26] Interestingly, the pattern can only be extended to a certain cluster size for both systems. For the mixed water–acetone system studied here, the pattern begins to break down at $n > 4$ for both $(H_2O)_n{\cdot}(C_3H_6O)_mH^+$ and $(H_2O)_n{\cdot}(C_3H_6O)_m{\cdot}CH_3CO^+$ cluster ions. Even though there are several possible reasons for the breaking down of this pattern, the formation the ring structure, which is known to exist in the condensed phase,[32] is a more plausible explanation.

B. Correlation of Metastable Decomposition Channels and Their Structures. For the following general discussion, the mixed cluster ion is written as $(A)_n{\cdot}(T)_mH^+$ (A ≡ H_2O or NH_3, T ≡ acetone, pyridine, or trimethylamine). In all cases considered, the molecule

(32) Davison, D. W. In *Water a Comprehensive Treatise: Clathrate Hydrates*: Franks, F., Ed.; Plenum: New York, 1972; Vol. 2.

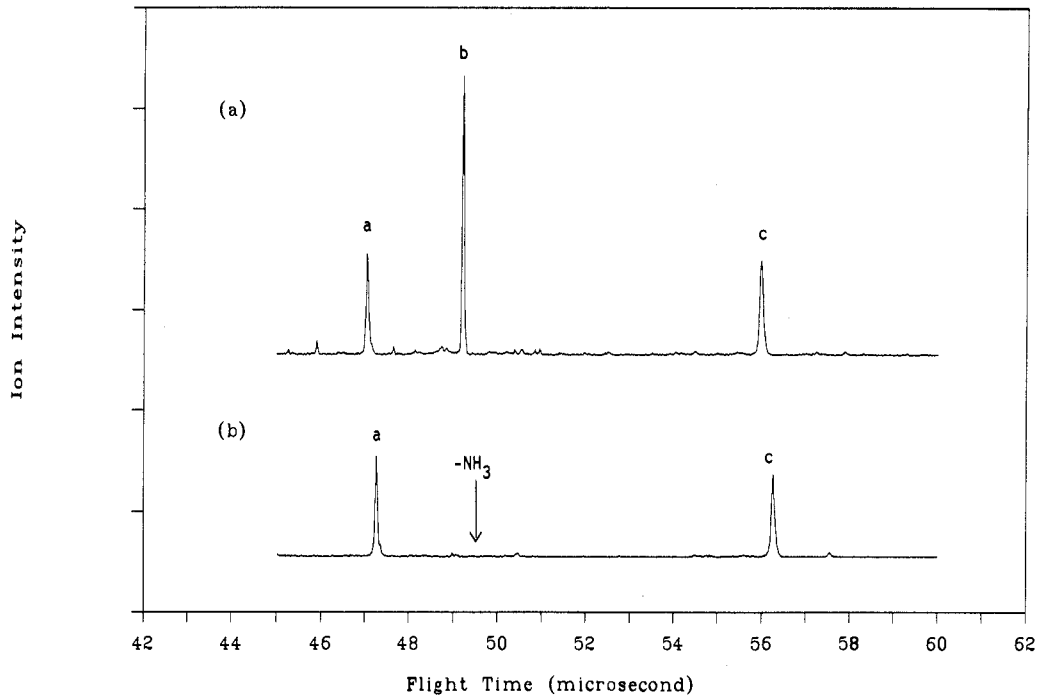

Figure 9. A metastable daughter ion cutoff potential study. Detailed discussion is in the text. (a) A metastable daughter ion TOF spectrum at U_t = 2550 V. The corresponding parent ions for peaks a–c are $(C_5H_5N)_3H^+$, $NH_3{\cdot}(C_5H_5N)_3H^+$, and $NH_3{\cdot}(C_5H_5N)_4H^+$. (b) A daughter ion TOF spectrum at U_t = 2300 V. Peak b is gone, indicating ammonia is lost from $NH_3{\cdot}(C_5H_5N)_3H^+$. Peaks a and c still exist, indicating pyridine is lost from $(C_5H_5N)_3H^+$ and $NH_3{\cdot}(C_5H_5N)_4H^+$.

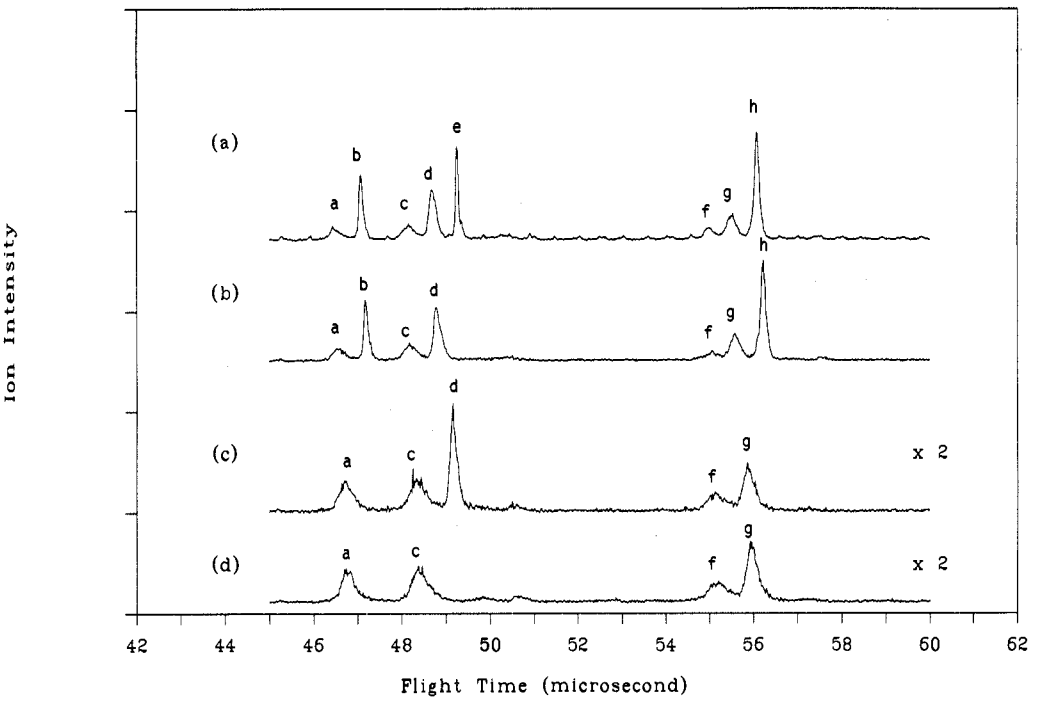

Figure 10. A CID daughter ion cutoff potential study. Detailed discussion is in the text. (a) A CID daughter ion TOF spectrum at U_t = 2550 V. The corresponding parent ions for these peaks are the following: peaks a and b from $(C_5H_5N)_3H^+$; peaks c, d, and e from $NH_3{\cdot}(C_5H_5N)_3H^+$; peaks f, g, and h from $NH_3{\cdot}(C_5H_5N)_4H^+$. (b) A CID daughter ion TOF spectrum at U_t = 2300 V. The daughter peak e is gone indicating only this channel corresponds to ammonia loss. (c) A CID daughter ion TOF spectrum at U_t = 1730 V. The daughter peaks b and h are gone indicating pyridine is lost. (d) A CID daughter ion TOF spectrum at U_t = 1621 V. The daughter peak d is gone showing ammonia and pyridine are lost. The assignments of the rest of the peaks are the following: peak a, two pyridine loss; peak c, two pyridine and one ammonia loss; peak f, three pyridine and one ammonia loss; peak g, two pyridine and one ammonia loss.

T has higher proton affinity than the corresponding A molecule, but no active hydrogen for forming the extended hydrogen-bonding network. In the case of one–one combination, i.e. $A{\cdot}H^+{\cdot}T$, the proton is more strongly bonded by T due to its higher proton affinity. Whenever there are two or more T molecules in the cluster ion, the most stable structure could be either a very stable protonated dimer core ion $T{\cdot}H^+{\cdot}T$, to which the other A or T is loosely bonded, or a $A{\cdot}H^+$ ion, to which the T molecules are strongly hydrogen bonded. The experimental results showing the existence of the core ions such as H_3O^+, $H_5O_2^+$, NH_4^+, $N_2H_7^+$, etc. in these mixed hydrogen-bonded systems suggest that the structure transition takes places before or when the hydrogen-bonding shell is fully closed. The detailed metastable and CID studies on these systems lead us to believe that there is a good

Table IV. Metastable and CID Channels of $(NH_3)_n((CH_3)_3N)_mH^+$ [a]

parent ion	metastable	CID	ratio[c]
$NH_3((CH_3)_3N)H^+$	$-NH_3$	$-NH_3$	1
$NH_3((CH_3)_3N)_2H^+$	$-NH_3$	$-NH_3$	1
		$-NH_3 + (CH_3)_3N$	0.57
$NH_3((CH_3)_3N)_3H^+$	$-NH_3$	$-NH_3$[b]	1
		$-NH_3 + (CH_3)_3N$	0.62
		$-NH_3 + 2(CH_3)_3N$	0.59
$NH_3((CH_3)_3N)_4H^+$	$-(CH_3)_3N$	$-(CH_3)_3N$	1
		$-NH_3 + 2(CH_3)_3N$	0.95
		$-NH_3 + 3(CH_3)_3N$	0.35
$NH_3((CH_3)_3N)_5H^+$	$-(CH_3)_3N$	$-(CH_3)_3N$	1
		$-2(CH_3)_3N$	0.38
		$-NH_3 + 3(CH_3)_3N$	0.33
		$-NH_3 + 4(CH_3)_3N$	0.24
$(NH_3)_2((CH_3)_3N)H^+$	$-NH_3$	$-NH_3$	1
		$-2NH_3$	0.45
$(NH_3)_2((CH_3)_3N)_2H^+$	$-NH_3$	$-NH_3$	1
		$-2NH_3$	0.51
		$-2NH_3 + (CH_3)_3N$	0.64
$(NH_3)_2((CH_3)_3N)_3H^+$	$-NH_3$	$-NH_3$	1
		$-2NH_3 + (CH_3)_3N$	0.34
		$-2NH_3 + 2(CH_3)_3N$	0.29
$(NH_3)_2((CH_3)_3N)_4H^+$	$-NH_3$	$-NH_3$	1
		$-NH_3 + (CH_3)_3N$	0.30
		$-2NH_3 + 2(CH_3)_3N$	0.29
		$-2NH_3 + 3(CH_3)_3N$	0.22
$(NH_3)_2((CH_3)_3N)_5H^+$	$-NH_3$	$-NH_3$[b]	1
		$-NH_3 + (CH_3)_3N$	0.67
		$-NH_3 + 2(CH_3)_3N$	0.40
		$-2NH_3 + 3(CH_3)_3N$	0.23
		$-2NH_3 + 4(CH_3)_3N$	0.22
$(NH_3)_2((CH_3)_3N)_6H^+$	$-(CH_3)_3N$	$-(CH_3)_3N$	1
		$-NH_3 + 2(CH_3)_3N$	0.41
		$-NH_3 + 3(CH_3)_3N$	0.38
		$-2NH_3 + 4(CH_3)_3N$	0.16
		$-2NH_3 + 5(CH_3)_3N$	0.10

[a] The results of metastable decompositions are from ref 26 and are listed here for the direct comparison with the CID results. $-NH_3$ denotes loss of ammonia; $-(CH_3)_3N$ denotes loss of pyridine; $-NH_3 + (CH_3)_3N$ denotes loss of ammonia and pyridine. [b] This channel is due to the metastable decomposition. [c] Normalized to the most intense daughter ion peak.

correlation between the transition of metastable channels and the transition of the cluster ion structures as discussed in the following.

For the mixed cluster ions ($n + m < 6$) discussed below, studies of the metastable decomposition process can provide information of the relative bonding strength in the mixed cluster ions by using the critical assumption of competitive shift. This can be understood on the basis of the following Born–Haber cycle:

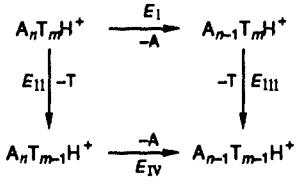

$E_1 + E_{III} = E_{II} + E_{IV}$ where E_1 to E_{IV} are the dissociation energies of corresponding cluster ions. The above equation does not hold if the cluster ion has more than one stable configuration and the energy barrier for the interconversion between different structures is higher than its dissociation energy. However, the assumption of a single cluster ion configuration does apply to most hydrogen-bonded systems even though a few exceptions have been found.[33] In particular, it can be applied to the present water–acetone and ammonia–pyridine systems since only one metastable peak is observed for all mixed cluster ions studied except $(H_2O)_2{\cdot}(C_3H_6O)_4H^+$. For the reason that the channel with lower dissociation energy is favored during metastable decomposition, the relative values of E_1 and E_{II} are obtained.[18,26,34] From the equation $E_1 + E_{III} = E_{II} + E_{IV}$, the relative values of E_{III} and E_{IV} are clear. It is seen from the above cycle that E_{III} and E_{IV} also reflect the binding energies of A and T molecules to the cluster ion $(A)_{n-1}{\cdot}(T)_{m-1}H^+$, so one can obtain the relative binding strength of A and T to cluster ion $(A)_{n-1}{\cdot}(T)_{m-1}H^+$ by studying the metastable decomposition of $(A)_n{\cdot}(T)_mH^+$. In other words, the loss of an A moiety from $(A)_n{\cdot}(T)_mH^+$ (i.e. $E_{II} > E_I$) implies that the bonding energy of T to $A_{n-1}{\cdot}T_{m-1}H^+$ is larger than that of A to $A_{n-1}{\cdot}T_{m-1}H^+$ (i.e. $E_{III} > E_{IV}$).

In the case of $H_2O{\cdot}(C_3H_6O)H^+$, our experimental result shows that water is lost in the metastable decomposition processes (see Table II) which means that acetone is more strongly bonded to the proton than water. It is consistent with the fact that the proton affinity of acetone is higher than that of water (Table I). In the case of $H_2O{\cdot}(C_3H_6O)_2H^+$, the loss of water in the metastable decomposition process, as shown in Table II, implies that the acetone molecule is more strongly bonded to $(C_3H_6O)H^+$. This finding is in agreement with the thermochemical data where the bond dissociation energies of $(C_3H_6O)H^+{\cdot}H_2O$ and $(C_3H_6O)H^+{\cdot}C_3H_6O$ have been reported to be 20.5 and 31.5 kcal/mol, respectively.[37]

The same argument can be applied to the cluster ions $NH_3{\cdot}(C_5H_5N)_mH^+$, $m = 1$–2. When $m = 1$, loss of ammonia indicates pyridine has a higher proton affinity. When $m = 2$, loss of ammonia is consistent with the fact that the bonding energy of $(C_5H_5N)H^+{\cdot}NH_3$, 17.3 kcal/mol,[37] is smaller than that of $(C_5H_5N)H^+{\cdot}C_5H_5N$, 23.7 kcal/mol.[35-37]

There are two possible structures for the cluster ion $NH_3{\cdot}(C_5H_5N)_2H^+$ (or $H_2O{\cdot}(C_3H_6O)_2H^+$): (1) by forming a very stable core ion $(C_5H_5N)_2H^+$ to which the ammonia molecule is loosely bonded (structure I-A); and (2) by breaking the stable ion

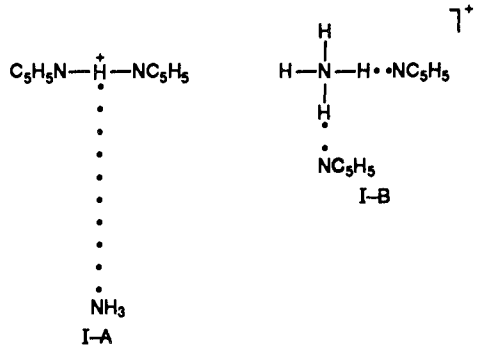

$(C_5H_5N)_2H^+$ and forming NH_4^+ to which two pyridine molecules are strongly hydrogen bonded (structure I-B). In the case where there is a molecular rearrangement occurring in the cluster ion within our observation time, study of the metastable decomposition does not indicate the most stable structure. The present CID study serves as a complementary method for determining the most stable configuration of a cluster ion. The experimental results (Table III) show that $NH_3{\cdot}(C_5H_5N)_2H^+$ does not lose a pyridine molecule during the high-energy (about 2.6 keV) collisions with nitrogen gas. Together, these findings indicate structure I-A is more stable than structure I-B for the cluster ion $NH_3{\cdot}(C_5H_5N)_2H^+$.

The same conclusion concerning the structure of $NH_3{\cdot}(C_5H_5N)_2H^+$ or $H_2O{\cdot}(C_3H_6O)_2H^+$ can also be seen from the metastable decomposition studies of $NH_3{\cdot}(C_5H_5N)_3H^+$ or $H_2O{\cdot}(C_3H_6O)_3H^+$. Although there are no thermochemical data of the binding energy for $(C_5H_5N)_2H^+{\cdot}NH_3$ to be compared with that of $(C_5H_5N)_2H^+{\cdot}C_5H_5N$ (12.6 kcal/mol[37]), the loss of an ammonia moiety from $NH_3{\cdot}(C_5H_5N)_3H^+$ during the metastable decomposition (see Table III) indicates the binding energy of $(C_5H_5N)_2H^+{\cdot}NH_3$ is less than 12.6 kcal/mol. On the basis of the argument of ion–dipole and ion–induced dipole interactions,

(33) Wei, S.; Tzeng, W. B.; Castleman, A. W., Jr. *J. Phys. Chem.* **1990**, *94*, 6927.
(34) Stace, A. J.; Moore, C. J. *J. Am. Chem. Soc.* **1983**, *105*, 1814. Stace, A. J. *J. Am. Chem. Soc.* **1984**, *106*, 2306.
(35) Meot-Ner, M. *J. Am. Chem. Soc.* **1984**, *106*, 1257.
(36) Holland, P. M.; Castleman, A. W., Jr. *J. Chem. Phys.* **1982**, *76*, 4195.
(37) Keesee, R. G.; Castleman, A. W., Jr. *J. Phys. Chem. Data Ref.* **1986**, *15*, 1011.

the smaller interaction is expected for ammonia since both dipole moment and polarizability of pyridine are larger than that of ammonia (Table I). This satisfactory explanation suggests that NH_3 is indeed loosely bonded to $(C_5H_5N)_2H^+$ (structure I-A), otherwise NH_3 will be more strongly bonded in $NH_3{\cdot}(C_5H_5N)_2H^+$ than C_5H_5N in $C_5H_5N{\cdot}(C_5H_5N)_2H^+$ if structure I-B is correct.

Now we consider $H_2O{\cdot}(C_3H_6O)_3H^+$ and $NH_3{\cdot}(C_5H_5N)_3H^+$. Two possible structures are the following (T ≡ C_3H_6O): (1) structure II-A (the positions of the outside H_2O may be different from the drawing), three acetone molecules bonded to the proton forming $(C_3H_6O)_3H^+$ (a T-shape structure has been proposed on the basis of an ab initio MO calculation by Yamabe et al.[38]) and the water molecule loosely bonded to $(C_3H_6O)_3H^+$; (2) structure II-B, the water molecule bonded to the proton forming H_3O^+ and three acetone molecules bonded to H_3O^+ and forming three O--H-O bonds.

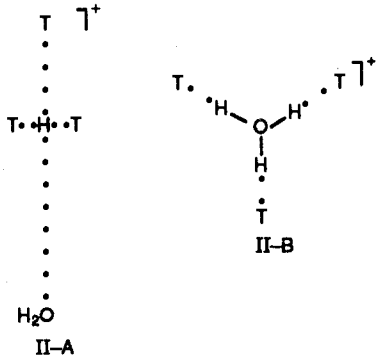

As seen from Figure 2, the magic number pattern gives an indication that H_3O^+ is the core ion to which three acetone molecules are hydrogen bonded. Our CID studies on this species provide further conclusive evidence that the structure is II-B since the water loss channel is pressure independent and the acetone loss channel increases as the pressure increases as seen in Figure 5. In other words, the water loss channel is only a metastable process which involves the intracluster molecular rearrangement from structure II-B to structure II-A and the loosely bonded water molecule is lost from II-A. Since the CID process proceeds at large values of internal energy, the dissociation rate of direct bond cleavage (loss of acetone) is much faster than isomerization (loss of water).[20,21] Subsequently, the acetone loss channel shows the pressure dependence.

Klots[39] pointed out that the metastable decomposition fraction of a particular cluster ion only depends on the measuring time window. It is not surprising that the measured dissociation fraction of the water loss channel remains unchanged since the time window of the cluster ion $H_2O{\cdot}(C_3H_6O)_3H^+$ is the same for all experiments.

As for mixed ammonia–pyridine, the CID study also leads to the conclusion that the ammonia loss from $NH_3{\cdot}(C_5H_5N)_3H^+$ is a purely metastable process for the following reasons: (1) the dissociation fraction of this channel stays almost unchanged (compare 10.7% for process 5 and 10.2% for process 9) when flowing collision gas (N_2) up to 0.02 sccm, whereas the fractions of the other dissociation channels increase considerably (from 7.0% to 14.2% for processes 4 and 7, 11.9% to 18.0% for processes 6 and 12); and (2) under multiple collision conditions, no process corresponding to the similar channel exists for the larger cluster ions $NH_3{\cdot}(C_5H_5N)_mH^+$, $m > 3$, for example, $NH_3{\cdot}(C_5H_5N)_4H^+ \not\rightarrow (C_5H_5N)_3H^+ + NH_3 + C_5H_5N$, $NH_3{\cdot}(C_5H_5N)_5H^+ \not\rightarrow (C_5H_5N)_3H^+ + NH_3 + 2C_5H_5N$. Recall the local minimum at $m = 2$ observed in the abundance distributions of $NH_3{\cdot}(C_5H_5N)_mH^+$ at different mixing ratios. The CID studies provide an explanation since no production of $NH_3{\cdot}(C_5H_5N)_2H^+$ is observed for the large mixed cluster ions as seen in Table III. Similarly, the fragmentation of large mixed clusters produces little $NH_3{\cdot}(C_5H_5N)_2H^+$ during the multiphoton ionization process which results in the observed local minimum. These findings can be explained on the basis of the structure transition between $m = 2$ and 3 for cluster ions $NH_3{\cdot}(C_5H_5N)_mH^+$ similar to the mixed system $H_2O{\cdot}(C_3H_6O)_mH^+$. First, the unchanged dissociation fraction of dissociation channel 5 (loss of ammonia only) during the CID process is due to the fact that ammonia is the solvation core ion, and the high-energy collision results in the loss of pyridine instead of ammonia. Second, the observation that the dissociation processes such as $NH_3{\cdot}(C_5H_5N)_4H^+ \not\rightarrow (C_5H_5N)_3H^+ + NH_3 + C_5H_5N$ do not exist under multiple collision conditions can be understood as following. After the pyridine loss from $NH_3{\cdot}(C_5H_5N)_4H^+$, the resultant product ion $NH_3{\cdot}(C_5H_5N)_3H^+$ is stable with its precursor's core ion, NH_4^+. Therefore, the loss of ammonia molecule from $NH_3{\cdot}(C_5H_5N)_3H^+$ or the overall channel of $NH_3{\cdot}(C_5H_5N)_4H^+ \not\rightarrow (C_5H_5N)_3H^+ + NH_3 + C_5H_5N$ will not open.

Interestingly, this structure transition is also implied by the transition of metastable decomposition channels of these mixed systems; i.e. the metastable dissociation pattern of the protonated cluster ions $H_2O{\cdot}(C_3H_6O)_mH^+$ and $NH_3{\cdot}(C_5H_5N)_mH^+$ switch from $m = 3$ to 4 (Tables II and III) since acetone and pyridine molecules are lost during the metastable decomposition when $m \geq 4$. First, we consider the cluster ion $NH_3{\cdot}(C_5H_5N)_4H^+$. The pyridine loss implies that the binding energy of $(C_5H_5N)_3H^+{\cdot}NH_3$ is larger than that of $(C_5H_5N)_3H^+{\cdot}C_5H_5N$ (measured value 13.6 kcal/mol[37]). The argument based on ion–dipole and ion–induced dipole interaction does not provide a satisfactory explanation for this case. A better explanation is that ammonia is bonded to the proton-forming NH_4^+ which is then bonded by three other C_5H_5N molecules forming three N--H-N hydrogen bonds (structure like I-B). Similarly, the fact that the metastable channel of $H_2O{\cdot}(C_3H_6O)_mH^+$ switches between $m = 3$ and 4 in the case of the mixed water–acetone system also implies that the structure at $m = 3$ is different from that at $m = 2$ which is consistent with the results of the CID studies.

This general correlation can be successfully applied to other similar systems such as mixed ammonia–trimethylamine, water–dimethyl ether cluster ions, etc. The transition of the metastable channel found in the mixed ammonia–trimethylamine cluster ion is between $m = 3$ and 4 which implies the structure changes at $m = 3$ and this is also supported by the present CID studies (Table IV). In the mixed cluster ions, $H_2O{\cdot}(CH_3OCH_3)_mH^+$, the metastable decomposition channel switches between $m = 2$ and 3 which suggests that the structure changes as early as $m = 2$; this finding is also consistent with the conclusion from other studies.[22,40]

Conclusion

The metastable decomposition study of the mixed cluster ions provides the relative binding strength of two species. For the small cluster ions of $A{\cdot}(T)_mH^+$ (A ≡ NH_3 or H_2O, T ≡ C_5H_5N or C_3H_6O), $m = 1$ and 2, the species (pyridine or acetone) with higher proton affinity is more strongly bonded to the proton. When $m > 3$, however, the species (ammonia or water) which has the smaller proton affinity is found to be the core ion to provide the maximum hydrogen-bonding sites. The CID studies give direct evidence for these structural assignments. And the change of the core ion is also reflected from the transition of the metastable decomposition channels of both mixed systems at $m = 3$–4. The ammonia or water loss from the cluster ion $NH_3{\cdot}(C_5H_5N)_3H^+$ or $H_2O{\cdot}(C_3H_6O)_3H^+$ during the metastable decomposition is a result of intracluster molecular rearrangement during the observable time window of the TOFMS.

Acknowledgment. Support by the U.S. Department of Energy, Grant No. DE-FGO2-ER60648, is gratefully acknowledged.

(38) Yamabe, S.; Minato, T.; Hirao, K. *Can. J. Chem.* **1983**, *61*, 2827.
(39) Klots, C. E. *Z. Phys. D* **1987**, *5*, 83. Klots, C. E. *J. Phys. Chem.* **1988**, *92*, 5864.
(40) Hiraoka, K.; Grimsrud, E. P.; Kebarle, P. *J. Am. Chem. Soc.* **1974**, *96*, 3359.